

## ELASTIC-PLASTIC STRESS ANALYSIS OF THERMOPLASTIC MATRIX LAMINATED COMPOSITE BEAMS

Hasan Çallıoğlu\*, N. Sinan Köksal\*\*, Necati Ataberk\*\*\*, İdris Kaynak\*\*\*\*

\* Department of Mechanical Engineering, Pamukkale University, Çamlık Denizli, Turkey.

\*\* Department of Mechanical Engineering, Celal Bayar University, Muradiye, Manisa, Turkey.

\*\*\* Sarayönü Vocational Training School, Selçuk University, Konya, Turkey.

\*\*\*\* Department of Mechanical Engineering, Dokuz Eylül University, Bornova, İzmir, Turkey.

**Abstract** - This study deals with an elastic-plastic behavior of woven steel fibers reinforced thermoplastic matrix laminated composite beam subjected to a bending moment. The beam consists of symmetric four orthotropic layers and its material is assumed to be strain hardening. The Tsai-Hill theory is used as a yield criterion in the solution. The Bernoulli-Euler hypotheses are utilized for small plastic deformations. The beam lay-up sequences are chosen as  $[0^{\circ}]_4$ ,  $[15^{\circ}/-15^{\circ}]_s$ ,  $[30^{\circ}/-30^{\circ}]_s$  and  $[45^{\circ}/-45^{\circ}]_s$ . The bending moment values that begin plastic flow at the upper and lower surfaces of the beam are carried out for various stacking sequences. The variations of the elastic, elastic-plastic and residual stress components versus increasing plastic region spread are given in tables and figures. The transverse displacement is obtained at the free end, numerically.

**Key Words** - Laminated composite beam, elastic-plastic stress analysis, small plastic deformation.

### 1. INTRODUCTION

There is a growing need to combine metals with polymeric composites in order to optimize the strength, weight and durability of components in aircraft, railway vehicle and spacecraft applications. Thermoplastic composites offer high specific stiffness and specific strength, improved interlaminar fracture toughness, increased impact resistance. Moreover, they may be remelted, reprocessed and reformed. Therefore, woven composite materials are being used as primary structural components in many applications such as automobile, construction, marine equipment, etc. Zhang and Harding [1] studied the elastic material properties of woven composites by numerical models. Ishikawa and Chou [2,3] studied one-dimensional linear and nonlinear micromechanical properties of woven composites. Cantwell [4] investigated the influence of stamping temperature on the properties of a glass mat thermoplastic composite.

The behavior of laminated composite structures can be effectively and efficiently tailored by changing the lay-up parameters. Icardi [5] presented a three-dimensional zig-zag theory for accurate stress and failure analysis of thick laminated and sandwich beams. Bhate et al. [6] presented a refined flexural theory for laminated composite beams subjected to mechanical and thermal loading. Rand [7] studied the relative

importance of the cross-sectional warping components in solid orthotropic beam undergoing a bending moment. Khdeir and Reddy [8] presented an exact solution for the bending of thin and thick cross-ply laminated beams by using the classical first-order, second-order and third-order theories in the analysis.

Brünig [9] presented an elastic-plastic analysis of work-hardening materials based on a quadratic approximation of the Tsai-Wu criterion. Dadras [10] presented an elastic-plastic stress analysis of plane strain pure bending of a strain-hardening curved beam. In that study only a linear hardening case has been analyzed. Chattopadhyay and Guo [11] developed non-linear structural design sensitivity analysis for structures undergoing elastoplastic deformation. Kojic et al. [12] analyzed elastic-plastic deformation of a beam, composite of layers with material orthotropic in elastic and plastic domains. Fares [13] presented a modified version of Reissner's mixed variational formula for investigating generalized non-linear thermoelasticity problem in composite laminated beam. Karakuzu and Özcan [14] carried out an elasto-plastic stress analysis on aluminum composite cantilever beam loaded by a single force at the free end and a uniformly distributed force at the upper surface by using an analytical solution. Sayman and Zor [15] investigated elastic-plastic stresses in a thermoplastic cantilever beam loaded uniformly.

In this study, an elastic-plastic stress analysis is carried out on woven steel fibers reinforced symmetric thermoplastic matrix laminated beams consisted of four layers subjected to a bending moment by using Bernoulli-Euler hypotheses. The Tsai-Hill theory is used as a yield criterion during the solution.

## 2. ELASTIC SOLUTION

Analysis of laminated beam subjected to pure bending can be developed from the Bernoulli-Euler theory [16]. According to this theory, the longitudinal normal strain at a distance  $z$  from the neutral surface is given as

$$\varepsilon_x = \frac{z}{\rho} \quad (1)$$

where  $\rho$  is the radius of curvature of the neutral surface during flexure, as shown in Figure 1.

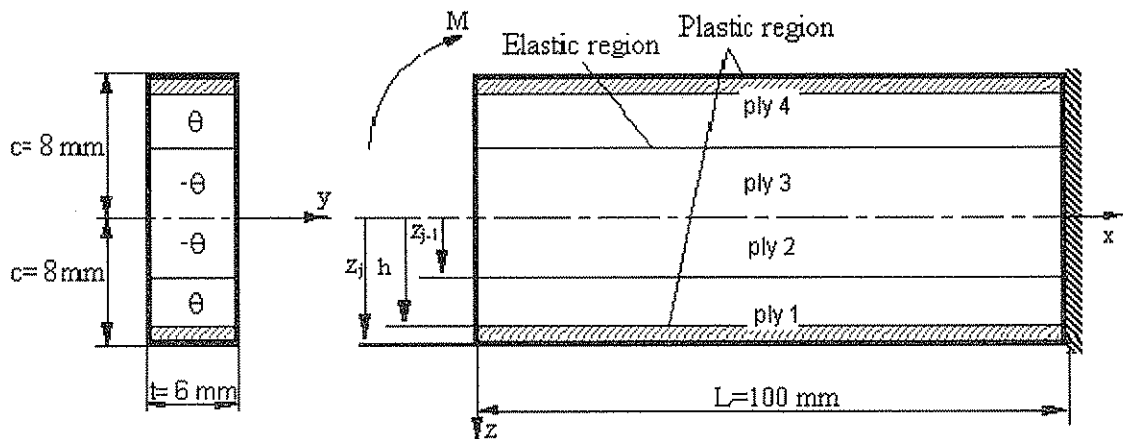


Figure 1. A laminated composite cantilever beam and its dimensions.

The longitudinal stress can be written by using,

$$(\sigma_x)_j = (E_x)_j \frac{z}{\rho} \quad (2)$$

where  $j$  is the plies number.  $(E_x)_j$  is the Young's modulus of  $j$ th ply.

The bending moment  $M$  can be related to the longitudinal stress because of the static equilibrium as,

$$M = 2 \int_0^c \sigma_x z t dz \quad (3)$$

or

$$M = \frac{2t}{3\rho} \sum_{j=1}^{\alpha/2} (E_x)_j (z_j^3 - z_{j-1}^3) \quad (4)$$

where  $2c$  and  $t$  are the height and thickness of the beam, and  $\alpha$  is the total number of plies and  $z_j$  is the distance from the neutral surface to the outside of the  $j$ th ply. The moment-curvature relation in a laminated beam can be evaluated as,

$$M = \frac{E_f I_{yy}}{\rho} \quad (5)$$

where  $I_{yy}$  is the inertia moment of the cross-section of the beam,  $E_f$  is the effective flexural modulus of the beam;  $E_f$  is written as,

$$E_f = \frac{1}{c^3} \sum_{j=1}^{\alpha/2} (E_x)_j (z_j^3 - z_{j-1}^3) \quad (6)$$

The stress component can be also written without using the radius of curvature;

$$(\sigma_x)_j = \frac{M}{E_f I_{yy}} (E_x)_j z = \frac{M z}{I_{yy}} \left[ \frac{(E_x)_j}{E_f} \right] \quad (7)$$

The strain-stress relation in the laminated composite beam is written as,

$$\begin{Bmatrix} \varepsilon_x \\ \varepsilon_z \\ \varepsilon_{xz} \end{Bmatrix} = \begin{bmatrix} \bar{a}_{11} & \bar{a}_{12} & \bar{a}_{16} \\ \bar{a}_{12} & \bar{a}_{22} & \bar{a}_{26} \\ \bar{a}_{16} & \bar{a}_{26} & \bar{a}_{66} \end{bmatrix} \begin{Bmatrix} \sigma_x \\ 0 \\ 0 \end{Bmatrix} \quad (8)$$

where  $\bar{a}_{ij}$  are the components of the compliance matrix [17]:

$$\begin{aligned} \bar{a}_{11} &= a_{11}r^4 + (2a_{12} + a_{66})r^2s^2 + a_{22}s^4 \\ \bar{a}_{12} &= a_{12}(r^4 + s^4) + (a_{11} + a_{22} - a_{66})r^2s^2 \\ \bar{a}_{22} &= a_{11}s^4 + (2a_{12} + a_{66})r^2s^2 + a_{22}r^4 \\ \bar{a}_{16} &= (2a_{11} - 2a_{12} - a_{66})sr^3 - (2a_{22} - 2a_{12} - a_{66})s^3r \\ \bar{a}_{26} &= (2a_{11} - 2a_{12} - a_{66})s^3r - (2a_{22} - 2a_{12} - a_{66})sr^3 \\ \bar{a}_{66} &= 2(2a_{11} + 2a_{22} - 4a_{12} - a_{66})r^2s^2 + a_{66}(r^4 + s^4) \end{aligned} \quad (9)$$

where  $r = \cos\theta$ ,  $s = \sin\theta$ ,  $a_{11} = 1/E_1$ ,  $a_{22} = 1/E_2$ ,  $a_{12} = -\nu_{12}/E_1$ ,  $a_{66} = 1/G_{12}$ . Eq. (2) can be also written in terms of the compliance matrix as,

$$(\sigma_x)_j = \frac{z}{\rho(\bar{a}_{11})_j} \quad (10)$$

### 3. ELASTIC-PLASTIC SOLUTION

In the elastic-plastic solution, the Bernoulli-Euler hypotheses are protected. According to these assumptions, plane sections remain plane and normal during flexure. Thus the unit strain in the longitudinal direction in the plastic region can be also written as,

$$\varepsilon_x = \frac{z}{\rho} \quad (11)$$

where  $\rho$  is the radius of the curvature of the beam.

The Tsai-Hill theory is used as a yield criterion due to the same yield strengths of the composite beams in tension and compression. X and Y are the yield strengths in the 1<sup>st</sup> and 2<sup>nd</sup> principal material directions. S is shear strength in 1-2 plane. It is assumed Z the yield strength in the 3<sup>rd</sup> direction to be equal to Y in the 2<sup>nd</sup> direction. It is also assumed that the shear strengths in the 1-3 and 2-3 planes to be equal to S in 1-2 plane. Under these assumptions, the yield condition according to this criterion can be evaluated as,

$$\frac{\sigma_1^2}{X^2} - \frac{\sigma_1\sigma_2}{X^2} + \frac{\sigma_2^2}{Y^2} + \frac{\tau_{12}^2}{S^2} = 1 \quad (12)$$

multiplying it by X gives the equivalent stress in the first principal material direction as,

$$\sigma_{eq} = \bar{\sigma} = \sqrt{\sigma_1^2 - \sigma_1\sigma_2 + \sigma_2^2 \frac{X^2}{Y^2} + \tau_{12}^2 \frac{X^2}{S^2}} \quad (13)$$

For a strain hardening material, the yield stress according to the Ludwik equation is written as,

$$\sigma_Y = \sigma_0 + K\varepsilon_p^n \quad (14)$$

where  $\sigma_0$  is nearly equal to X which is the yield strength in the first principal material direction, K, n and  $\varepsilon_p$  are the plasticity constant, strain-hardening parameter and equivalent plastic strain, respectively. In the plastic region, the equations of equilibrium are written as,

$$\begin{aligned} \frac{\partial \sigma_x}{\partial x} + \frac{\partial \tau_{xz}}{\partial z} &= 0 \\ \frac{\partial \tau_{xz}}{\partial x} + \frac{\partial \sigma_z}{\partial z} &= 0 \end{aligned} \quad (15)$$

After integration of the first equation  $\sigma_x$  is determined as  $C(z)$ . As a result of this, at any section, in the plastic region  $\sigma_x$  is only a function of z. The stress components in the principal material directions for the orientation angle  $\theta$  are written as,

$$\sigma_1 = \sigma_x r^2, \quad \sigma_2 = \sigma_x s^2, \quad \tau_{12} = -\sigma_x rs \quad (16)$$

where  $r=\cos\theta$ ,  $s=\sin\theta$ . Substituting them in Eq. (13) gives the yield strength for the orientation angle  $\theta$ ,

$$X_1 = \frac{X}{N} \quad (17)$$

where,

$$N = \sqrt{r^4 - s^2 r^2 + \frac{X^2 s^4}{Y^2} + \frac{X^2 s^2 r^2}{S^2}} \quad (18)$$

The plastic strain increments in the material directions can be obtained by using the potential function  $f = \bar{\sigma} - \sigma_Y(\epsilon_p)$  [18] as,

$$\begin{Bmatrix} d\epsilon_1^p \\ d\epsilon_2^p \\ d\epsilon_{12}^p \end{Bmatrix} = \begin{Bmatrix} \frac{\partial f}{\partial \sigma_1} d\lambda \\ \frac{\partial f}{\partial \sigma_2} d\lambda \\ \frac{\partial f}{\partial \tau_{12}} d\lambda \end{Bmatrix} \quad (19)$$

The total strain increments in the principal material directions are the summation of the elastic and plastic strain increments as [19],

$$\begin{aligned} d\epsilon_1 &= d\epsilon_1^e + d\epsilon_1^p = a_{11} d\sigma_1 + a_{12} d\sigma_2 + \frac{2\sigma_1 - \sigma_2}{2\sigma_Y} d\lambda \\ &\quad - \sigma_1 + \frac{2\sigma_2 X^2}{Y^2} \\ d\epsilon_2 &= d\epsilon_2^e + d\epsilon_2^p = a_{12} d\sigma_1 + a_{22} d\sigma_2 + \frac{2\sigma_2 - \sigma_1}{2\sigma_Y} d\lambda \\ &\quad + \frac{2\sigma_1 X^2}{Y^2} \\ d\epsilon_{12} &= d\epsilon_{12}^e + d\epsilon_{12}^p = \frac{a_{66} d\tau_{12}}{2} + \frac{2\tau_{12} X^2}{2\sigma_Y S^2} d\lambda \end{aligned} \quad (20)$$

The  $\sigma_x$  stress component for the orientation angle  $\theta$  can be written in the form of strain hardening as,  $\sigma_x = \sigma_Y / N$  and  $d\lambda$  is equal to the equivalent plastic increment  $d\epsilon_p$ . Putting  $\sigma_1$ ,  $\sigma_2$  and  $\tau_{12}$  into Eq. (20) and integrating them produces

$$\begin{aligned} \epsilon_1 &= a_{11}\sigma_1 + a_{12}\sigma_2 + \frac{2r^2 - s^2}{2N} \epsilon_p + C_5 \\ \epsilon_2 &= a_{12}\sigma_1 + a_{22}\sigma_2 + \frac{-r^2 + 2s^2}{2N} \frac{X^2}{Y^2} \epsilon_p + C_6 \\ \epsilon_{12} &= \frac{a_{66}\tau_{12}}{2} - \frac{2rs}{2N} \frac{X^2}{S^2} \epsilon_p + C_7 \end{aligned} \quad (21)$$

At the elastic and plastic boundary, elastic and plastic strain components are equal. By using this relation and writing  $\epsilon_p$  is zero at the boundary determines  $C_5$ ,  $C_6$  and  $C_7$

integration constants. The strain components in the principal material directions for the elastic region can be written as,

$$\begin{Bmatrix} \varepsilon_1 \\ \varepsilon_2 \\ \varepsilon_{12} \end{Bmatrix} = \begin{bmatrix} r^2 & s^2 & 2rs \\ s^2 & r^2 & -2rs \\ -rs & rs & r^2 - s^2 \end{bmatrix} \begin{Bmatrix} \varepsilon_x \\ \varepsilon_z \\ \varepsilon_{xz} \end{Bmatrix} \quad (22)$$

$$\begin{aligned} \varepsilon_1 &= \sigma_x (\bar{a}_{11} r^2 + \bar{a}_{12} s^2 + \bar{a}_{16} rs) \\ \varepsilon_2 &= \sigma_x (\bar{a}_{11} s^2 + \bar{a}_{12} r^2 - \bar{a}_{16} rs) \end{aligned} \quad (23)$$

$$\varepsilon_{12} = \sigma_x \left( -\bar{a}_{11} rs + \bar{a}_{12} rs + \frac{\bar{a}_{16}}{2} (r^2 - s^2) \right)$$

where  $\sigma_x = X_1$  which is the yield strength of a ply for the orientation angle  $\theta$ . Equating the strain components at the boundary of the elastic and plastic regions gives the integration constants. Then the strain components in the plastic region are written as,

$$\begin{aligned} \varepsilon_1 &= \sigma_x (a_{11} r^2 + a_{12} s^2) + X_1 [(\bar{a}_{11} - a_{11}) r^2 + (\bar{a}_{12} - a_{12}) s^2 + \bar{a}_{16} rs] + \frac{2r^2 - s^2}{2N} \varepsilon_p \\ \varepsilon_2 &= \sigma_x (a_{12} r^2 + a_{22} s^2) + X_1 [(\bar{a}_{11} - a_{22}) s^2 + (\bar{a}_{12} - a_{12}) r^2 - \bar{a}_{16} rs] + \frac{-r^2 + 2s^2 \frac{X^2}{Y^2}}{2N} \varepsilon_p \\ \varepsilon_{12} &= -\frac{\sigma_x}{2} a_{66} rs + X_1 \left( -\bar{a}_{11} rs + \bar{a}_{12} rs + \frac{\bar{a}_{16}}{2} (r^2 - s^2) + \frac{a_{66}}{2} rs \right) - \frac{2rs \frac{X^2}{S^2}}{2N} \varepsilon_p \end{aligned} \quad (24)$$

The strain components in the  $x$  and  $z$  directions are obtained by using the transformation formula,

$$\begin{Bmatrix} \varepsilon_x \\ \varepsilon_z \\ \varepsilon_{xz} \end{Bmatrix} = \begin{bmatrix} r^2 & s^2 & -2rs \\ s^2 & r^2 & 2rs \\ rs & -rs & r^2 - s^2 \end{bmatrix} \begin{Bmatrix} \varepsilon_1 \\ \varepsilon_2 \\ \varepsilon_{12} \end{Bmatrix} \quad (25)$$

They are determined as

$$\varepsilon_x = \bar{a}_{11} \sigma_x + B_1 \varepsilon_p, \quad \varepsilon_z = \bar{a}_{12} \sigma_x + B_2 \varepsilon_p, \quad \varepsilon_{xz} = \frac{\bar{a}_{16}}{2} \sigma_x + B_3 \varepsilon_p \quad (26)$$

where

$$\begin{aligned} B_1 &= \frac{2r^4 - 2r^2 s^2 + 2s^4 \frac{X^2}{Y^2} + 4r^2 s^2 \frac{X^2}{S^2}}{2N} \\ B_2 &= \frac{2r^2 s^2 - s^4 - r^4 + 2r^2 s^2 \frac{X^2}{Y^2} - 4r^2 s^2 \frac{X^2}{S^2}}{2N} \end{aligned} \quad (27)$$

$$B_3 = \frac{3r^3s - rs^3 - 2rs^3 \frac{X^2}{Y^2} + (-2r^3s + 2rs^3) \frac{X^2}{S^2}}{2N}$$

The  $\sigma_x$  stress component in the elastic region varies linearly in terms of the curvature of the radius as,

$$\sigma_x = \frac{z}{\rho \bar{a}_{11}} \quad (28)$$

Therefore, the distance between the plastic region and the x-axis are equal to h as seen from Figure 1.

At the yield point,  $\sigma_x$  is equal to  $X_1$  and  $X_1 = \frac{h}{\rho \bar{a}_{11}}$ , hence, the curvature of the radius is determined as,

$$\rho = \frac{h}{X_1 \bar{a}_{11}} \quad (29)$$

### 3.1. Displacement Components

#### i) Elastic Case

The  $\sigma_x$  stress component in the laminated beam is written as,

$$\sigma_x = E_x \varepsilon_x = \frac{z}{\rho \bar{a}_{11}} \quad (30)$$

writing  $\frac{1}{\rho \bar{a}_{11}} = d$ ,  $\sigma_x$  becomes

$$\sigma_x = d z \quad (31)$$

and strain component can be written in terms of displacement components u and w,

$$\varepsilon_x = \frac{\partial u}{\partial x} = \bar{a}_{11} \sigma_x = d \bar{a}_{11} z$$

$$\varepsilon_z = \frac{\partial w}{\partial z} = \bar{a}_{12} \sigma_x = d \bar{a}_{12} z \quad (32)$$

$$\varepsilon_{xz} = \frac{1}{2} \left( \frac{\partial u}{\partial z} + \frac{\partial w}{\partial x} \right) = \frac{\bar{a}_{16}}{2} \sigma_x = d \frac{\bar{a}_{16}}{2} z$$

where u and w are the longitudinal and transverse displacements, respectively.

After integration the above equations, the displacement components are obtained in terms of the integration constants. The boundary conditions at the fixed end

$u = w = \frac{\partial w}{\partial x} = 0$  at  $x=L$  and  $z=0$ , give the integration constants. Then the displacements are found as,

$$\begin{aligned}
u &= d \bar{a}_{11} z x + \frac{d \bar{a}_{16} z^2}{2} - d \bar{a}_{11} l z \\
w &= \frac{\bar{a}_{12} d z^2}{2} - \frac{d \bar{a}_{11} x^2}{2} + d \bar{a}_{11} l x - \frac{d \bar{a}_{11} l^2}{2}
\end{aligned} \tag{33}$$

### ii) Elastic-Plastic Case

For small deformations, the relation between the strain and displacement components can be written as,

$$\varepsilon_x = \frac{\partial u}{\partial x} = \frac{z}{\rho} = \bar{a}_{11} \sigma_x + B_1 \varepsilon_p \tag{34}$$

or

$$\frac{z}{\rho} = \bar{a}_{11} \frac{\sigma_0 + K \varepsilon_p^n}{N} + B_1 \varepsilon_p \tag{35}$$

similarly,  $\varepsilon_z$  is related to  $w$  as,

$$\varepsilon_z = \frac{\partial w}{\partial z} = \bar{a}_{12} \sigma_x + B_2 \varepsilon_p \tag{36}$$

$$\text{where } \sigma_x = \frac{\sigma_y}{N} = \frac{\sigma_0 + K \varepsilon_p^n}{N}.$$

The integration of  $u$  and  $w$  gives the displacement components as

$$\begin{aligned}
u &= \frac{z}{\rho} x + C_1(z) \\
w &= \int_h^z \left( \bar{a}_{12} \frac{\sigma_0 + K \varepsilon_p^n}{N} + B_2 \varepsilon_p \right) dz + C_2(x)
\end{aligned} \tag{37}$$

$u$  and  $w$  must satisfy the following relation as,

$$\varepsilon_{xz} = \frac{1}{2} \left( \frac{\partial u}{\partial z} + \frac{\partial w}{\partial x} \right) = \frac{\bar{a}_{16}}{2} \sigma_x + B_3 \varepsilon_p \tag{38}$$

where  $\varepsilon_p$  is a function of  $z$ , as a result of this, this relation is obtained

$$\frac{x}{\rho} + \frac{dC_1(z)}{dz} + \frac{dC_2(x)}{dx} = 2 \left( \frac{\bar{a}_{16}}{2} \frac{\sigma_0 + K \varepsilon_p^n}{N} + B_3 \varepsilon_p \right) \tag{39}$$

and

$$\frac{x}{\rho} + \frac{dC_1(z)}{dz} + \frac{dC_2(x)}{dx} - \left( \bar{a}_{16} \frac{\sigma_0 + K \varepsilon_p^n}{N} + 2B_3 \varepsilon_p \right) = 0 \tag{40}$$

$$\frac{dC_1(z)}{dz} - \bar{a}_{16} \frac{\sigma_0 + K \varepsilon_p^n}{N} - 2B_3 \varepsilon_p = G_1 \tag{41}$$

$$\frac{x}{\rho} + \frac{dC_2(x)}{dx} = K_1$$

$$K_1 + G_1 = 0$$



$C_2$  is obtained as

$$C_2 = K_1 x - \frac{x^2}{2\rho} + C_3 \quad (42)$$

$w$  is much higher than  $u$ , therefore  $w$  is calculated only,

$$w = \int_h^z \left( \bar{a}_{12} \frac{\sigma_0 + K \varepsilon_p^n}{N} + B_2 \varepsilon_p \right) + K_1 x - \frac{x^2}{2\rho} + C_3 \quad (43)$$

If the plastic region expands in the first and second plies, at the boundary of the elastic and plastic regions; displacement components and their slopes must be equal,

$$(w)_e = (w)_p \text{ and } \left( \frac{\partial w}{\partial x} \right)_e = \left( \frac{\partial w}{\partial x} \right)_p \text{ at } x=L \text{ and } z=h$$

using these relations, they are found as,

$$K_1 = \frac{L}{\rho}, \quad C_3 = \left| \bar{a}_{12} \frac{h^2}{2\rho \bar{a}_{11}} \right| - \frac{L^2}{2\rho} - \left| \bar{a}_{12} \frac{\sigma_0 h}{N} \right| \quad (44)$$

where subscript 1 is the first ply number.

$w_1$  is equal to  $w_2$  at the boundary of first and second plies. The transverse displacement component in the second ply can be written as,

$$w = \int_{c/2}^z \left( \left| \bar{a}_{12} \frac{\sigma_0 + K \varepsilon_p^n}{N} \right|_2 + |B_2|_2 \varepsilon_p \right) dz + \int_h^{c/2} \left( \left| \bar{a}_{12} \frac{\sigma_0 + K \varepsilon_p^n}{N} \right|_1 + |B_2|_1 \varepsilon_p \right) dz + \frac{L}{\rho} x - \frac{x^2}{2\rho} + \left| \bar{a}_{12} \frac{h^2}{2\rho \bar{a}_{11}} \right| - \frac{L^2}{2\rho} - \left| \bar{a}_{12} \frac{\sigma_0}{N} \right| h \quad (45)$$

This integration is performed numerically. First, the Eq. (35) is solved numerically by the Newton-Raphson method, and then  $\varepsilon_p$  is obtained. By using  $\varepsilon_p$ , the integration (Eq. 45) is carried out by Newton-Cotes Formulas numerically. Subsequently, the transverse displacement component at the lower surface ( $x=0$  and  $z=c$ ) is obtained approximately.

### 3.2. Determination of Bending Moment

The moment at any section can be evaluated according to the boundary of the plastic region. The moment of the  $\sigma_x$  stress component has to be equal to the bending moment  $M$ . If the plastic region is expanded only in the first ply, the bending moment

$$M = 2 \left[ \int_{z=0}^{c/2} \frac{z}{\rho |\bar{a}_{11}|_2} z t dz + \int_{z=c/2}^h \frac{z}{\rho |\bar{a}_{11}|_1} z t dz + \int_{z=h}^c \left| \frac{X + K \varepsilon_p^n}{N} \right|_1 z t dz \right] \quad (46)$$

where  $t$  is the thickness of the beam. The curvature is evaluated from the yield strength of the second ply (Eq.10) as,

$$\sigma_x = X_1 = \frac{h}{|\bar{a}_{11}|_1 \rho}, \quad \rho = \frac{h}{|\bar{a}_{11}|_1 X_1} \quad (47)$$

where  $X_1$  is the yield strength of the first ply and is equal to  $X/N$ . This integration is performed numerically by Newton-Cotes Formulas.

If the plastic region is spread from the lower surface into the second ply, the bending moment

$$M = 2 \left[ \int_{z=0}^h \frac{z}{\rho |\bar{a}_{11}|_2} z t dz + \int_{z=h}^{c/2} \left| \frac{X + K \varepsilon_p^n}{N} \right|_2 z t dz + \int_{z=c/2}^c \left| \frac{X + K \varepsilon_p^n}{N} \right|_1 z t dz \right] \quad (48)$$

where indices show the mechanical properties of the plies. The above integration is carried out numerically, by using Newton-Cotes Formulas.

#### 4. RESIDUAL STRESSES

If  $h$  is known, the bending moment  $M$  in Eqs. (46) and (48) can be calculated. Afterwards, elastic and elastic-plastic stress components of  $\sigma_x$  for a each ply can be calculated from following equations, respectively:

$$(\sigma_x)_e = \frac{M z}{I} \left[ \frac{(E_x)_j}{E_f} \right] \quad (49)$$

$$(\sigma_x)_p = \frac{\sigma_Y}{N} = \left| \frac{\sigma_0 + K \varepsilon_p^n}{N} \right|_j \quad (50)$$

The superposition of the elastic and elastic-plastic stresses gives the residual stress components as,

$$(\sigma_x)_r = (\sigma_x)_p - (\sigma_x)_e \quad (51)$$

where subscripts r, p and e indicate residual stress, elastic-plastic stress and elastic stress, respectively.

#### 5. DISCUSSION ON A SAMPLE

A polyethylene thermoplastic matrix laminated composite cantilever beam reinforced woven steel fibers symmetrically is analyzed analytically. The mechanical properties and yield strengths of a ply are given in Table 1.

**Table 1.** Mechanical properties and yield strengths of a ply.

$E_1$ (MPa)	$E_2$ (MPa)	$G_{12}$ (MPa)	$\nu_{12}$	X=Y (MPa)	Z (MPa)	S (MPa)	K (MPa)	n	$V_f$
13000	13000	400	0.46	22	16	11	115	0.69	0.09

Lay-up sequences are chosen as  $[0^\circ]_4$ ,  $[15^\circ/-15^\circ]_s$ ,  $[30^\circ/-30^\circ]_s$  and  $[45^\circ/-45^\circ]_s$ . Bending moments initiate plastic yielding at the same values on the upper and lower surfaces. As seen in Table 2, the bending moment starting plastic yielding is found to be highest for the  $[0^\circ]_4$  orientation, as 5632 Nmm. When the orientation angle is chosen as  $[15^\circ/-15^\circ]_s$ ,  $[30^\circ/-30^\circ]_s$  and  $[45^\circ/-45^\circ]_s$ , its value decreases gradually. The lowest one is  $[45^\circ/-45^\circ]_s$ , and it is 5037 Nmm.

**Table 2.** Bending moment values starting plastic yielding in the laminated beam.

Orientation angles	$[0^\circ]_4$	$[15^\circ/-15^\circ]_s$	$[30^\circ/-30^\circ]_s$	$[45^\circ/-45^\circ]_s$
Bending moment (Nmm)	5632	5464	5168	5037

When the plastic region is expanded from the lower or upper surfaces towards the neutral surface, plastic, elastic and residual stresses are given at Table 3. The stress components and plastic flow are given at the lower surfaces and the residual stress components are also given at the elastic and plastic boundary per  $h$ , where  $h$  is the distance between the plastic region and neutral surface. The elastic-plastic and elastic stress components of  $\sigma_x$  are found to be maximum at the upper and lower surfaces. The magnitude of the residual stress component of  $\sigma_x$  is greatest at the upper and lower surfaces. However, when plastic region is further expanded from the lower or upper surfaces towards the neutral surface, the residual stress component of  $\sigma_x$  becomes the highest at the elastic and plastic boundary.  $\sigma_x$  residual stress component is found to be maximum for  $[0^\circ]_4$  orientation. The plastic flow is found to be highest for  $[45^\circ/-45^\circ]_s$  orientation as  $40.6 \cdot 10^{-3}$ . The equivalent stress of the plastic stresses in the principal material direction is also given at the table. The equivalent stress is found to be highest, 34.60 MPa, for  $[45^\circ/-45^\circ]_s$  orientation.

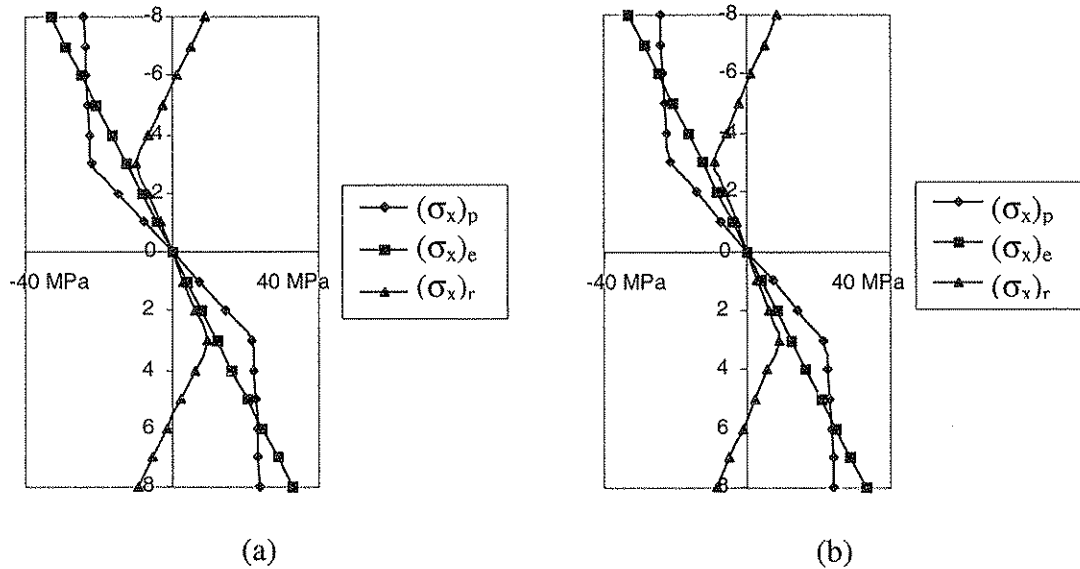
**Table 3.** Plastic, elastic and residual stresses at the lower surface and the residual stress at the elastic and plastic boundaries.

Orientation angles	M (Nmm)	h (mm)	$\epsilon_p \cdot 10^{-3}$	At the lower surface			In principal material axes $(\sigma_{eq})_p$ (MPa)	At the elastic-plastic boundary $(\sigma_x)_r$ (MPa)
				$(\sigma_x)_p$ (MPa)	$(\sigma_x)_e$ (MPa)	$(\sigma_x)_r$ (MPa)		
$[0^\circ]_4$	6310	7	0.2	22.34	24.65	-2.31	22.34	0.43
	6927	6	0.5	22.62	27.06	-4.44	22.62	1.71
	7484	5	0.9	22.94	29.23	-6.29	22.94	3.73
	7991	4	1.6	23.35	31.21	-7.86	23.35	4.80
	8470	3	2.7	23.93	33.08	-9.15	23.93	9.59
	8984	2	4.9	24.91	35.09	-10.18	24.91	13.23
	9810	1	11.4	27.26	38.32	-11.06	27.26	17.21
$[15^\circ/-15^\circ]_s$	6132	7	0.4	21.88	23.95	-2.07	22.55	0.38
	6758	6	1.1	22.33	26.40	-4.07	23.02	1.54
	7345	5	1.9	22.84	28.69	-5.85	23.55	3.41
	7907	4	3.3	23.51	30.89	-7.38	24.23	5.90
	8483	3	5.6	24.46	33.14	-8.68	25.21	8.92
	9175	2	10.2	26.06	35.84	-9.78	26.86	12.38
	10438	1	24.2	29.91	40.77	-10.86	30.83	16.25
$[30^\circ/-30^\circ]_s$	5808	7	0.6	20.84	22.68	-1.84	22.71	0.34
	6421	6	1.6	21.41	25.08	-3.67	23.33	1.38
	7011	5	2.9	22.06	27.39	-5.33	24.04	3.07
	7598	4	5.0	22.90	29.68	-6.78	24.95	5.35
	8229	3	8.4	24.10	32.14	-8.04	26.26	8.13
	9036	2	15.5	26.13	35.30	-9.17	28.48	11.36
	10537	1	37.0	31.03	41.40	-10.37	33.81	15.01
$[45^\circ/-45^\circ]_s$	5663	7	0.7	20.35	22.13	-1.78	22.75	0.32
	6266	6	1.7	20.94	24.47	-3.54	23.41	1.32
	6850	5	3.2	21.62	26.76	-5.14	24.17	2.95
	7435	4	5.5	22.49	29.04	-6.55	25.14	5.16
	8073	3	9.2	23.73	31.53	-7.80	26.53	7.85
	8898	2	17.0	25.85	34.76	-8.91	28.90	10.99
	10515	1	40.6	30.95	41.07	-10.12	34.60	14.54

The distribution of the elastic-plastic, elastic and residual stresses for  $h=3$  mm is shown in Figures 2 (a)-(d) for  $[0^\circ]_4$ ,  $[15^\circ/-15^\circ]_s$ ,  $[30^\circ/-30^\circ]_s$  and  $[45^\circ/-45^\circ]_s$  orientations, respectively. The magnitudes of the plastic and elastic stress components of  $\sigma_x$  are found to be maximum at the upper and lower surfaces. However, the  $\sigma_x$  residual stress component is found to be the highest at the elastic and plastic boundary as shown in Figure 2 (a) for  $[0^\circ]_4$  orientation.

The distributions of the  $\sigma_x$  stress components for  $[15^\circ/-15^\circ]_s$ ,  $[30^\circ/-30^\circ]_s$  and  $[45^\circ/-45^\circ]_s$  orientations are similar to  $[0^\circ]_4$  orientation as shown in Figures 2 (b)-(d), respectively. Similarly, plastic and elastic stresses are found to be maximum at the upper and lower surfaces, whereas the residual stress component is found to be highest at the boundary of the elastic and plastic regions.

When plastic region is expanded step by step from the lower or upper surfaces towards the neutral surface, that is when  $h$  is 7, 5, 3 and 1 mm etc., the distributions of the  $\sigma_x$  residual stress components along the cross-sections of the beams are shown in Figure 3 for the  $[0^\circ]_4$  orientation. As shown in Figure 3, the magnitudes of the residual stress components are found to be highest at the upper and lower surfaces. When the plastic region is further expanded, the magnitudes of the residual stress components become the highest at the boundary of the elastic and plastic regions.  $\sigma_x$  residual stress components for  $[15^\circ/-15^\circ]_s$ ,  $[30^\circ/-30^\circ]_s$  and  $[45^\circ/-45^\circ]_s$  orientations are shown in Figures 4-6, respectively. As shown in all the figures,  $\sigma_x$  residual stress component is found to be highest at the upper and lower surfaces; whereas, when the plastic region is further expanded the  $\sigma_x$  residual stress components reach the highest at the boundary of the elastic and plastic regions.



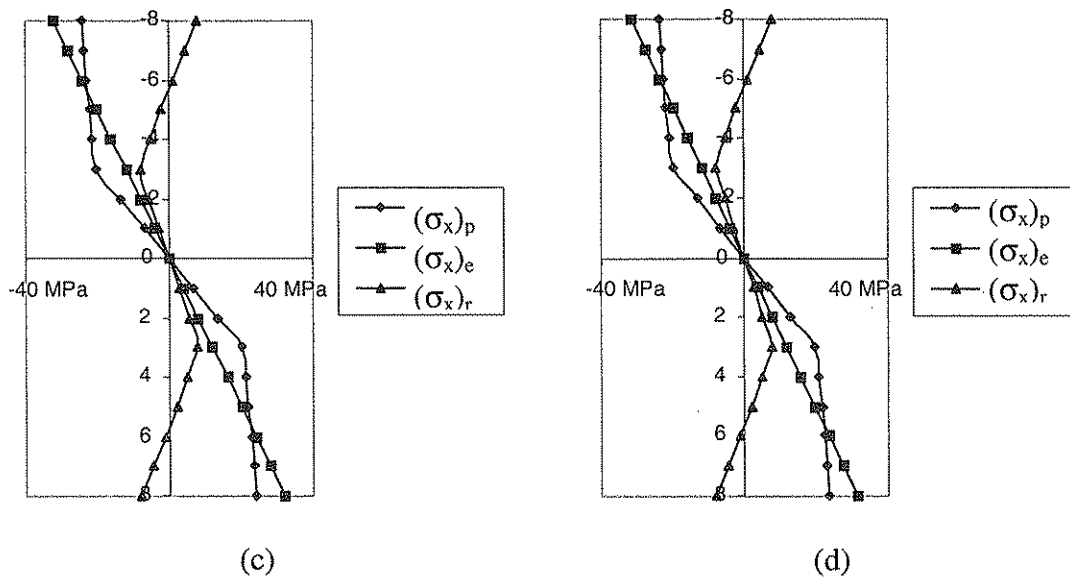


**Figure 2.** The distributions of the elastic-plastic, elastic and residual stress components of  $\sigma_x$  for the a)  $[0^\circ]_4$ ; b)  $[15^\circ/-15^\circ]_s$ ; c)  $[30^\circ/-30^\circ]_s$ ; d)  $[45^\circ/-45^\circ]_s$  orientations,  $h=3$  mm.

### 5.1. Transverse Displacement

The transverse displacement,  $w$ , is calculated numerically, for the plastic region expanded in both first and second plies until  $h=4, 3$  and  $2$  mm is given in Table 4. According to Table 4,  $w$  is found to be highest for  $[45^\circ/-45^\circ]_s$  orientation. When lay-up sequences are chosen as  $[30^\circ/-30^\circ]_s$ ,  $[15^\circ/-15^\circ]_s$  and  $[0^\circ]_4$ ,  $w$  decreases gradually.

**Table 4.** Transverse displacements of the laminated beam.

Orientation angles	h (mm)	w (mm)	Orientation angles	h (mm)	w (mm)
$[0^\circ]_4$	4	-2.12	$[30^\circ/-30^\circ]_s$	4	-12.74
	3	-2.83		3	-17.00
	2	-4.24		2	-25.52
$[15^\circ/-15^\circ]_s$	4	-5.86	$[45^\circ/-45^\circ]_s$	4	-15.93
	3	-7.82		3	-21.26
	2	-11.73		2	-31.91

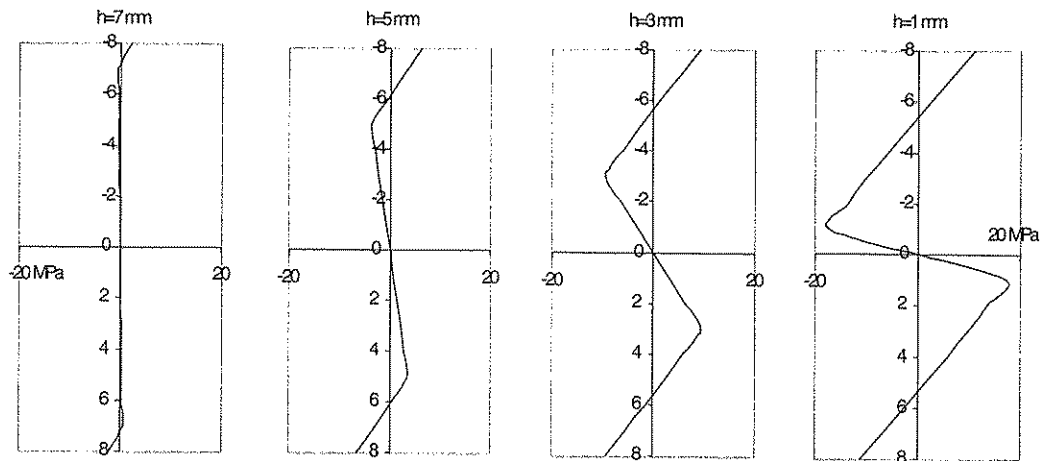


Figure 3. The distribution of  $\sigma_x$  residual stress component for the  $[0^\circ]_4$  orientation.

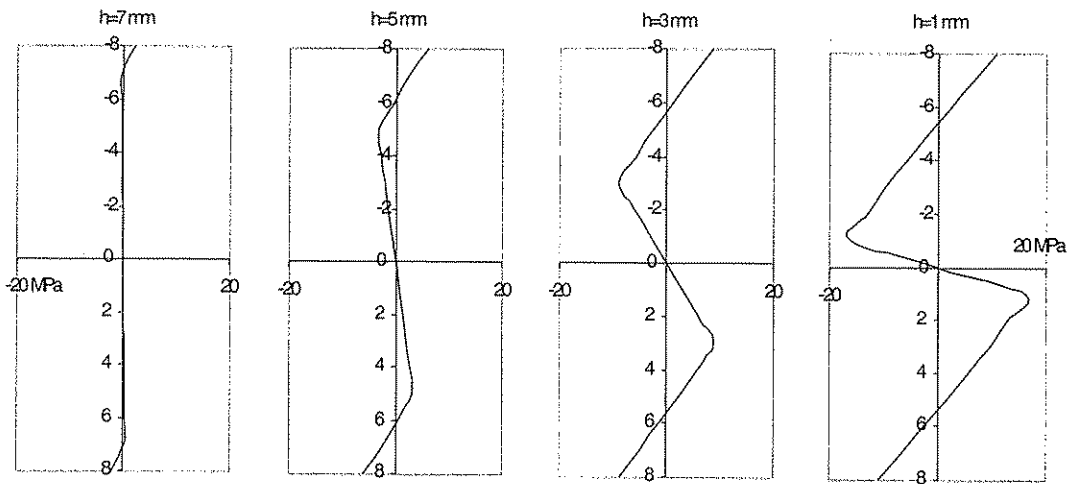


Figure 4. The distribution of  $\sigma_x$  residual stress component for the  $[15/-15^\circ]_s$  orientation.

## 6. CONCLUSION

In this study, elastic-plastic stress distribution on a symmetric woven steel fiber reinforced thermoplastic matrix laminated composite beam subjected to a bending moment is analyzed analytically. The following conclusions are made assuming that composite material is strain hardening and Bernoulli–Euler hypotheses are valid:

The plastic region starts first at the upper and the lower surfaces of the laminated beam for the chosen orientations.

The elastic-plastic solution gives the highest  $\sigma_x$  stress at the upper and lower surfaces of the beams for all orientations.

The magnitudes of the  $\sigma_x$  residual stress components are obtained to be highest at the upper and lower surfaces. When the plastic region is further increased, the  $\sigma_x$  residual stress components become the highest at the boundary of the elastic and plastic regions.

The magnitudes of the  $\sigma_x$  residual stress components are to be the highest for  $[0^\circ]_4$  orientation comparing to  $[15^\circ/-15^\circ]_s$ ,  $[30^\circ/-30^\circ]_s$  and  $[45^\circ/-45^\circ]_s$  orientations for further expansion of the plastic region.

The magnitude of the equivalent plastic strain is found to be the highest for  $[45^\circ/-45^\circ]_s$  orientation.

The transverse displacement,  $w$ , is found to be highest for  $[45^\circ/-45^\circ]_s$  orientation at the free end.

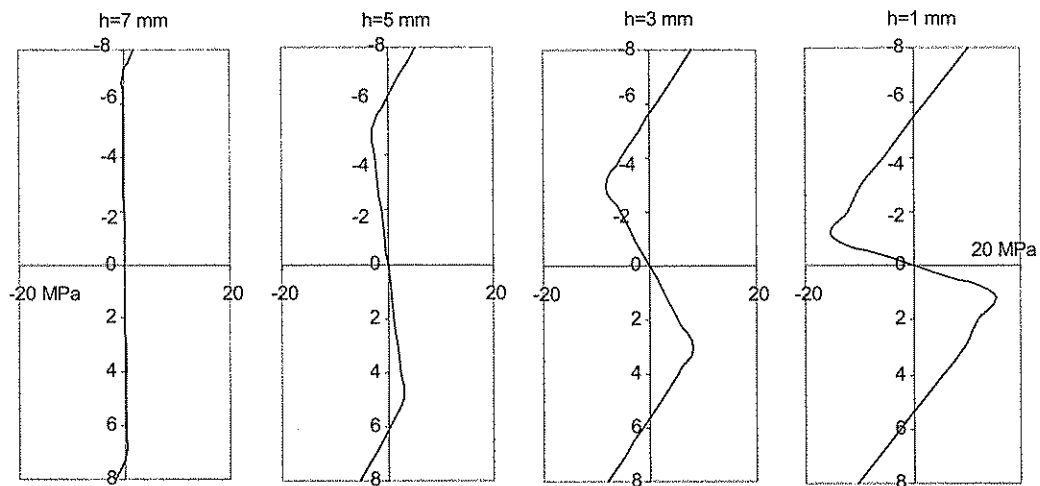


Figure 5. The distribution of  $\sigma_x$  residual stress component for the  $[30^\circ/-30^\circ]_s$  orientation.

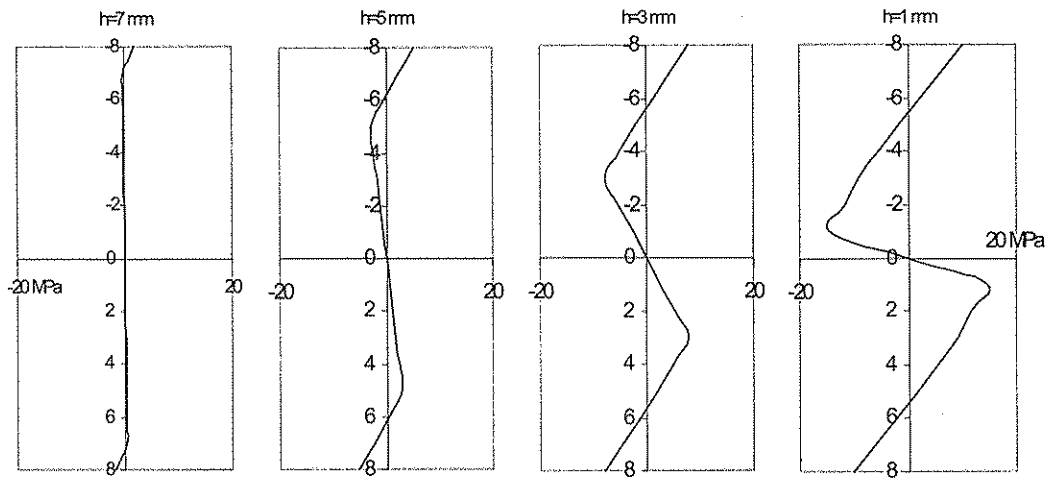


Figure 6. The distribution of  $\sigma_x$  residual stress component for the  $[45^\circ/-45^\circ]_s$  orientation.

## 7. REFERENCES

1. Zhang, Y.C. and Harding, J.A., 'A numerical micromechanics analysis of the mechanical properties of a plain weave composite' *Computers & Structures* 36(5), 839-44, 1990.
2. Ishikawa, T. and Chou, T.W., 'One-dimensional micromechanical analysis of woven fabric composites' *AIAA J* 21(12), 1714-1721, 1983.

3. Ishikawa, T. and Chou, T.W., 'Nonlinear behavior of woven fabric composites' *Journal of Composite Materials* **17**, 399-413, 1983.
4. Cantwell, W.J., 'The influence of stamping temperature on the properties of a glass mat thermoplastic composite' *Journal of Composite Materials* **30**(10), 1266-81, 1996.
5. Icardi, U., 'A three-dimensional zig-zag theory for analysis of thick laminated beams' *Composite Structures* **52**, 123-135, 2001.
6. Bhate, S.R., Nayak, U.N. and Patki, A.V., 'Deformation of composite beam using refined theory' *Computers & Structures* **54**, 541-546, 1995.
7. Rand, O., 'On the importance of cross-sectional warping in solid composite beams' *Composite Structures* **49**, 393-397, 2000.
8. Khdeir, A.A. and Reddy, J.N., 'An exact solution for the bending of thin and thick cross-ply laminated beams' *Composite Structures* **37**, 195-203, 1997.
9. Brüning, M., 'Nonlinear analysis and elastic-plastic behavior of anisotropic structures' *Finite Elements in Analysis and Design* **20**, 155-177, 1995.
10. Dadras, P., 'Plane strain elastic-plastic bending of a strain-hardening curved beam' *International Journal of Mechanical Sciences* **43**, 39-56, 2001.
11. Chattopadhyay, A. and Guo, R., 'Structural design sensitivity analysis for composites undergoing elastoplastic deformation' *Mathl. Comput. Modelling* **22**(2), 83-105, 1995.
12. Kojik, M., Zivkovic, M. and Kojik, A., 'Elastic-plastic analysis of orthotropic multilayered beam' *Computers & Structures* **57**, 205-211, 1995.
13. Fares, M.E., 'Generalized non-linear thermoelasticity for composite laminated structures using a mixed variational approach' *International Journal of Non-Linear Mechanics* **35**, 439-446, 2000.
14. Karakuzu, R. and Özcan, R., 'Exact solution of elasto-plastic stresses in a metal-matrix composite beam of arbitrary orientation subjected to transverse loads' *Composite Science and Technology* **56**, 1383-1389, 1997.
15. Sayman, O. and Zor, M., 'Elastic-plastic stress analysis and residual stress in a woven steel fiber reinforced thermoplastic composite cantilever beam loaded uniformly' *Journal of Reinforced Plastics and Composites* **19**(13), 1078-1092, 2000.
16. Gibson, R.F., *Principles of Composite Material Mechanics*, McGraw-Hill, Singapore, 1994.
17. Jones, R.M., *Mechanics of Composite Materials*, Taylor & Francis, Philadelphia, 1999.
18. Owen, D.R.J. and Hinton, E., *Finite Elements in Plasticity*, Pineridge Press, Swansea, 1980.
19. Chakrabarty, J., *Theory of Plasticity*, McGraw-Hill, Singapore, 1987.